^{10}Be(d, p)^{11}Be and the ^{10}Be(d, α)^{8}Li Reactions*

D. R. Goosman† and R. W. Kavanagh

California Institute of Technology, Pasadena, California 91109

(Received 15 December 1969)

Beryllium enriched to 5% in ^{10}Be has been extracted from neutron-irradiated carbon, and has been used for targets in nuclear spectroscopy. The cross section for the production of ^{8}Li via deuteron bombardment of ^{10}Be has been measured from 0.67 to 3.0 MeV, and the production cross section of ^{11}Be has been measured from 2.3 to 12 MeV. The yield for both reactions varies smoothly with bombarding energy, and no resonance in ^{12}B is seen. From magnetic spectroscopy of the ^{10}Be(d, p) reaction, the mass excess of ^{11}Be is found to be 20.174 ± 0.007 MeV (^{12}C = 0) and the excitation energy of the first excited level to be 318 ± 7 keV. The angular distribution of protons populating the 318-keV level is an $l_n = 1$ pattern, implying $J^\pi = \frac{1}{2}^-$ or $\frac{3}{2}^-$.

1. INTRODUCTION

When ^{10}Be is bombarded with deuterons with $E \leq 12$ MeV, the following reactions can occur, with the indicated Q values:

$$^{10}\text{Be} + d \rightarrow {}^{12}\text{B} + \gamma \quad Q = 12.37 \text{ MeV},$$
$$^{11}\text{B} + n \quad Q = 9.00 \text{ MeV},$$
$$^{8}\text{Li} + \alpha \quad Q = 2.37 \text{ MeV},$$
$$^{9}\text{Be} + t \quad Q = -0.56 \text{ MeV},$$
$$^{11}\text{Be} + p \quad Q = -1.73 \text{ MeV}.$$

The last two of these have recently been investigated by Auton *et al.*[1] From the proton angular distributions, they assigned $J^\pi = \frac{1}{2}^+$ and $\frac{1}{2}^-$, respectively, to the ground and first excited states of ^{11}Be, confirming an earlier prediction by Talmi and Unna that the $2s_{1/2}$ shell-model state lies below the $1p_{1/2}$ state in this region. Previous measurements[2,3] of the ^{9}Be(t, p)^{11}Be reaction indicated positive parity and $J = \frac{1}{2}$, $\frac{3}{2}$, or $\frac{5}{2}$ for the ground state, but the additional complexity from the spin-$\frac{3}{2}$ target nucleus precluded a unique spin assignment. A definite positive-parity assignment was made by Alburger *et al.*,[4] from the existence of allowed β decay to positive-parity states of ^{11}B.

The present investigation was carried out prior to the appearance of the work of Auton *et al.*,[1] and in part had similar objectives. In particular, the angular distribution of protons from ^{10}Be(d, p)^{11}Be to the first excited state of ^{11}Be, as described in Sec. 3, confirms the assignment $J^\pi = \frac{1}{2}^-$ to the 318-keV state. The excitation functions for production of the radionuclides ^{8}Li and ^{11}Be were also measured in the ranges $0.67 \leq E_d \leq 3.0$ MeV and $2.3 \leq E_d \leq 12$ MeV, respectively. The results, described in Secs. 2 and 3, are remarkably smooth and show no evidence for resonances involving the compound nucleus ^{12}B in the corresponding region, where $T = 2$ states may be expected.

Details regarding the target preparation and composition are contained in the appendix.

2. ^{10}Be(d, α)^{8}Li REACTION

A. Introduction

Using the crude value[5] of 25.1 ± 1 MeV for the mass excess of ^{12}Be, together with the position of the lowest $T = 1$ level in ^{12}C at 15.1 MeV,[5] and a Coulomb-energy term proportional to $Z(Z-1)/A^{1/3}$, the position of the lowest $T = 2$ level in ^{12}B may be estimated to lie between 12 and 14 MeV in excitation energy, i.e., at less than 2 MeV above the ^{10}Be + d threshold at 12.37 MeV. The ^{10}Be(d, α)^{8}Li excitation function was investigated for possible resonances in this region because it has a favorable Q value (+2.37 MeV), and because the high-energy β rays from the decay of ^{8}Li are easily detected and are not obscured by reactions involving the ^{9}Be or ^{16}O in the target. The (d, α) reaction is isospin forbidden in both the entrance and exit channels, of course, but previously reported results have shown that $T = \frac{3}{2}$ levels in the compound nucleus can be seen in the ^{12}C(p,p), ^{16}O(p,p), ^{20}Ne(p,p), and ^{36}Ar(p,p) reactions,[6] and $T = 2$ in the ^{6}Li(d,p) and ^{6}Li(d, α) reactions[7]; all of these are isospin forbidden in entrance and exit channels. In the present case, the lowest $T = 2$ state in ^{12}B presumably has $J^\pi = 0^+$, and is therefore not observable in ^{10}Be + d reactions. Higher $T = 2$ states with $J^\pi \neq 0^+$ are not J^π forbidden in this entrance channel.

B. Apparatus

A BeO target, 75 ± 8 μg/cm^2 thick (1.36 ± 0.35 μg/cm^2 of ^{10}Be), on a 5.7 ± 0.4-mg/cm^2 Pt foil, was mounted on a stainless-steel holder and placed in a small chamber (shown in Fig. 1) with the BeO upstream on the foil. The entire chamber was contained in the well of a plastic scintillator

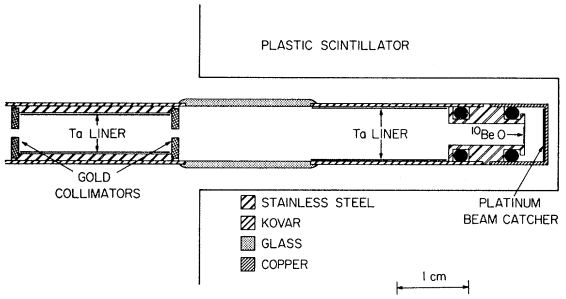

FIG. 1. The target chamber used to measure the (d, α) and the (d, p) excitation functions. Air cooling was provided for the beam catcher. The beam-catcher region was evacuated through slots (not shown) machined in the stainless-steel holder. The gold collimators defined a 1.5-mm beam spot on the target.

(Pilot B, 12.7 cm diam by 10.2 cm deep), to detect the β rays from the decay of ^{8}Li.

Photomultiplier pulses were amplified and stored in two halves of a 400-channel pulse-height analyzer. The beam was directed on target for one ^{8}Li mean life (1.23 sec), followed by a 0.4-sec delay, a counting period of 1.23 sec in one half of the analyzer, and then a second 1.23-sec counting period in the other half. Pulses between 6 and 10 MeV were counted during both the counting periods by a scaler, and during the second period only by a second scaler. Other scalers monitored the stability of the timing cycle by counting clock pulses, and the charge accumulated during the fixed number of beam-on cycles was measured. Despite the fact that it is not quite correct to normalize to charge for a fixed number of cycles to determine the cross section, the error incurred was negligible, since at least 20 cycles were used to determine the yield at each energy, and at least 3 cycles were run before starting data storage. The reproducibility of the β-ray yield for the entire 20 cycles for a fixed charge was better than 2%. Beam-energy fluctuations were negligible compared with the target thickness.

C. Results

The yields recorded by the two scalers as a function of deuteron energy are shown in Fig. 2. The ratio of counts in the two scalers should be 3.72 as long as the β rays originate from a nucleus with a mean life of 1.23 sec. This was the case within 2% for $E_d \leq 2.3$ MeV. Above 2.3 MeV, this ratio decreases because of the appearance of the ^{10}Be$(d, p)^{11}$Be(β^-) channel, which has a threshold at 2.1 MeV, and also results in high-energy β rays but with a longer mean life (19.6 sec). The dashed line in Fig. 2 is the continuation of the (d, α) cross section, and the difference between the data points

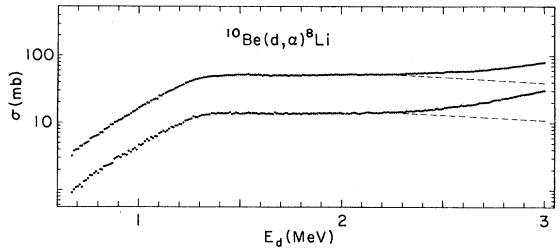

FIG. 2. The yield of ^{8}Li β radioactivity from ^{10}Be(d, α) ^{8}Li, in the apparatus of Fig. 1. The upper curve results from data accumulated during two mean lives after target irradiation, and the lower curve is from the second of those mean lives (τ=1.23 sec). The cross-section scale applies to the upper curve and its dashed extension, as explained in the text. α particles populating both the ground and 0.98-MeV states of ^{8}Li contribute to the yield.

and the dashed line is due to the (d, p) reaction; the required separation of the two reaction yields is readily made, since the mean lives are well known. The three prestorage cycles were insufficient for the ^{11}Be activity to reach equilibrium, but this causes an uncertainty of less than 1% in the extracted (d, α) cross section shown by the dashed line in Fig. 2. This figure should not be used to infer the (d, p) cross section, which is given correctly in Fig. 3.

The possibility of producing appreciable ^{8}Li by the ^{7}Li(d, p) reaction is ruled out by the marked difference between the shape of the excitation function near 1 MeV of Fig. 2 and that measured[8] for the ^{7}Li$(d, p)^{8}$Li reaction, and by other evidence (see Appendix B) that there is very little ^{7}Li on these targets. No other deuteron-induced reaction can make ^{8}Li at these energies. It may be noted that only the ground and first excited states of ^{8}Li contribute β radioactivity, since the higher states decay by neutron emission.

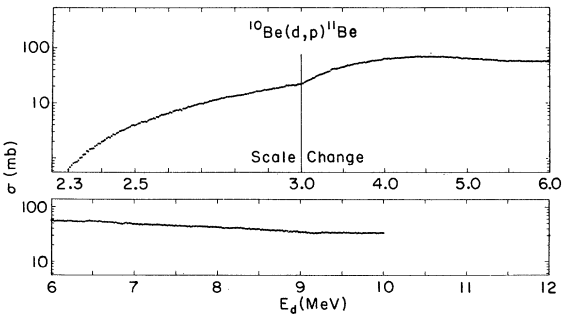

FIG. 3. The yield of ^{11}Be radioactivity from ^{10}Be(d, p) ^{11}Be, from data recorded during two ^{11}Be lifetimes (τ=19.6 sec) starting 6.6 sec after irradiation. Protons populating both the ground and 0.318-MeV states of ^{11}Be contribute to the yield. The target was 12 ±1.6 keV thick at 3 MeV.

The target thickness was measured with a NaI scintillation spectrometer, by comparing the yield of 4.44-MeV γ rays from the ^{9}Be$(\alpha, n\gamma)^{12}$C reaction at $E_\alpha = 4.55$ MeV and $\theta = 90°$ with the yield from a weighed ^{9}Be metal target in the same geometry. This metal foil was 50 ± 5 μg/cm^2 thick, representing an α-particle energy loss of 40 ± 6 keV. According to the measurements of Bonner *et al.*,[9] the ^{9}Be$(\alpha, n\gamma)^{12}$C cross section near $\theta_\gamma = 90°$ and $E_\alpha = 4.55$ MeV does not change rapidly enough with bombarding energy to cause additional uncertainty in the target-thickness measurement described here. In this way, the surface density of ^{9}Be in the BeO target could be determined to $\pm 10\%$, and thus the ^{10}Be to $\pm 25\%$, in view of the ratio of ^{10}Be/^{9}Be given in Appendix A. The timing efficiency of the cycle, i.e., the ratio of ^{8}Li decays occurring during both counting periods to the number of decays occurring during the entire cycle, is given by

$$\frac{(e^{T_b}-1)\,(e^{T_c}-1)}{T_b\,(e^{T_b+T_d+T_c}-1)},$$

where T_b, T_c, and T_d are, respectively, the beam-on, counting, and delayed periods, all normalized to the mean life of ^{8}Li. This ratio was 0.41 ± 0.01. Including an uncertainty of 33% for the absolute efficiency of the plastic scintillator in the geometry used, the absolute uncertainty of the vertical scale of Fig. 2 is about 43%.

As is evident from Fig. 2, no resonance in ^{12}B is seen. Because of the target thickness, a resonance less than 10 keV wide with an integrated strength of less than 35 ± 15 eV b would have been missed for most of the energy region covered by Fig. 2. The measurements were terminated at 3 MeV because of the growing dominance of the (d, p) reaction.

3. ^{10}Be$(d, p)^{11}$Be REACTION

A. Excitation Function

The study of this reaction had two objectives, to seek possible compound resonances in ^{12}B above 3-MeV deuteron energy, and to obtain an excitation function to guide the choice of bombarding energy at which to seek protons populating levels in ^{11}Be. For purposes of studying proton angular distributions and comparing them with distorted-wave calculations, an energy region free of sharp resonances is desirable.

Here again one would hope to locate $T = 2$ levels in ^{12}B, with a better chance of success than in the (d, α) reaction, because the (d, p) reaction is isospin forbidden in the entrance channel only, and the target thickness decreases with increasing bombarding energy.

The required excitation function was measured with the same apparatus as in the (d, α) reaction, except that the timing cycle was adjusted to correspond to the 19.6-sec mean life[5] of ^{11}Be. The delay period was increased to 6.6 sec to allow the ^{8}Li to decay to a negligible value. The data were taken in the same manner as described above, and the ratio of counting rates in the two scalers corresponded to a mean life within 2% of 19.6 sec for $E_d \geq 2.5$ MeV. Small corrections for cosmic-ray background were made for $E_d \leq 2.5$ MeV. The scaler bias was set at 6 MeV to eliminate effects of low-energy β rays, which dominated the spectrum below 2 MeV. The phototube was gated off during the beam-on time at bombarding energies above about 8 MeV, to avoid difficulties from the extremely high prompt counting rate. The results are shown in Fig. 3. The curve corresponding to the second counting period is not shown, since it runs parallel to the curve of Fig. 3. The uncertainty in the vertical scale is again about 43%, because of the same causes discussed in the (d, α) section. In addition to the scale uncertainty, there may be a relative error of about 10% in the ratio of cross sections taken from extreme ends of the excitation function shown in Fig. 3. Like the (d, α) yield, this curve is remarkable for its smoothness. The sensitivity for seeing a resonance less than about 7 keV wide is 12 ± 5 eV b for the integrated strength.

B. Spin of the 0.318-MeV Level in ^{11}Be

To measure proton angular distributions to the ground and first excited levels of ^{11}Be, a bombarding energy of 6 MeV was somewhat arbitrarily selected, since indeed there is no resonance structure to be concerned with, and the outgoing proton energy is sufficiently high (3 MeV) near the forward angles. At higher energies, the kinematic separation of contaminant groups becomes less favorable; above 10 MeV, the cross section is significantly lower, and (d, p) reactions in the platinum foil become bothersome.

Outgoing protons from a 84 ± 8-μg/cm^2 BeO target on 5.7-mg/cm^2 Pt were analyzed by a 61-cm-radius magnetic spectrometer, using a silicon detector at the focal plane. A thin foil in front of the detector enabled separation of α^{++} from protons in the pulse-height spectrum. The target was biased at +300 V and an electron-suppressor ring at −300 V preceded the target.

The proton profiles taken with reflection geometry at 153° and transmission geometry at 25° are shown in Fig. 4. In both cases the acceptance angles in the θ and ϕ directions were 1 and 6°, respectively, and the focal-plane aperture was set for an energy resolution of 0.28%. The peaks labeled ^{10}Be are due to the ^{9}Be$(d, p)^{10}$Be reaction,

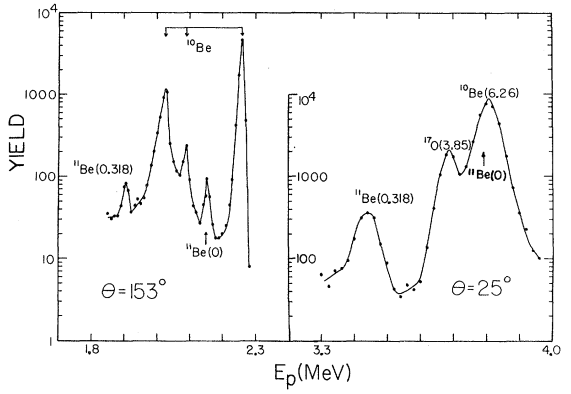

FIG. 4. The energy distribution of protons from 6-MeV deuteron bombardment of a BeO target. At $\theta_L = 153°$, the ^{10}Be$(d,p_0)^{11}$Be peak is located about 100 keV below the ^{9}Be(d,p_2) peak, which serves as an internal calibration.

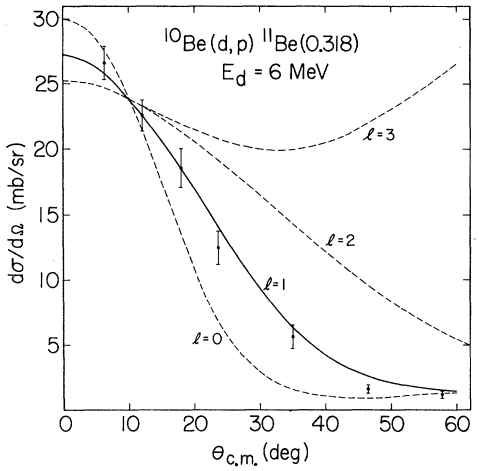

FIG. 5. The angular distribution of protons populating the 0.318-MeV level in ^{11}Be. Optical-model predictions are shown by the solid and dashed lines.

and those labeled ^{11}Be, to ^{10}Be$(d, p)^{11}$Be.

The points shown for $\theta = 153°$ in Fig. 4 are not equally spaced in energy or momentum. In particular, some of the points shown on the low-energy sides of the two ^{11}Be peaks are taken in 5-keV steps, or half of the 10-keV average step size. Although the two ^{11}Be peaks might at first glance appear to be broader than the ^{10}Be peak near 2.25 MeV, in fact their widths are about the same.

The ^{11}Be(0) peak in Fig. 4 is situated about 100 keV below the ^{10}Be($E_x = 5.959$) peak. Information recently summarized by Alburger *et al.*[10] on the levels of ^{10}Be indicate that the 5.959-MeV "level" is really two levels, one at 5958.3 ± 0.3 keV and one at 5959.9 ± 0.6 keV. No matter which of these two levels is the one seen in Fig. 4, that peak corresponds to an excitation energy of 5.9592 ± 0.0013 MeV. Since the ^{9}Be and the ^{10}Be in the target were thoroughly mixed, the ^{10}Be doublet and the ^{11}Be(0) peaks in Fig. 4 provide a measure of the mass excess of ^{11}Be, almost independent of target thickness, incident beam energy, and angle effects. Taking from Fig. 4 uncertainties of 5 keV in the location of the ^{11}Be(0) peak, 4 keV in the location of the ^{10}Be(5.959) doublet, 3% or 3 keV in the dispersion of the magnetic spectrometer, and combining them with the 1.3-keV uncertainty in the energy of the ^{10}Be doublet, one infers that the mass excess for the ground state of ^{11}Be is 20.174 ± 0.007 MeV (^{12}C = 0). The mass excesses of ^{10}Be, ^{2}H, and ^{1}H cancel out in the calculation. This value is in agreement with the previously reported value[2,5] of 20.181 ± 0.015 MeV, measured with the ^{9}Be$(t, p)^{11}$Be reaction.

The profile taken at 25° in Fig. 4 exhibits a resolution of 70 keV, attributable entirely to the straggle of the incident beam traversing the 5.7-mg/cm^2 Pt foil. With a thinner target (200 ± 20-μg/cm^2 BeO on 1.25-mg/cm^2 Pt), the resolution in transmission geometry was reduced to 35 keV, but this was still insufficient to resolve the ^{11}Be(0) peak from the nearby ^{10}Be and ^{17}O peaks at forward angles.

Protons populating the 0.318-MeV level in ^{11}Be were well resolved, however, and their angular distribution was measured in the forward hemispere, using the ^{10}Be target on the thin Pt backing. The results are shown in Fig. 5. At each angle, the protons were scanned over a 200-keV energy range, substantially greater than the 35-keV width of the proton group, in order to determine the small continuum background underlying the peak. The error bars in Fig. 5 reflect the uncertainty in this correction as well as counting statistics. The ^{9}Be content of this target was measured in the manner described in Sec. 2C. The ^{10}Be content of the target was known to ±25%, and this is the uncertainty in the cross-section scale of Fig. 5.

Distorted-wave optical-model predictions are shown for several l_n values, and the data are consistent only with the $l_n = 1$ pattern. The predictions are from the code JULIE[11,12] with no spin-orbit terms included, using optical parameters taken from Hodgson,[13] as listed in Table I. The optical potential used was of the form

$$\frac{V + iW}{1 + \exp\left[(r - r_0 A^{1/3})/a\right]} .$$

The assignment $l_n = 1$ agrees with that reported by Auton *et al.*[1] According to the results of the ^{9}Be $(t, p)^{11}$Be reaction,[3] the spin of this level is $\frac{1}{2}^-$, $\frac{3}{2}^-$, $\frac{5}{2}^-$, or $\frac{7}{2}^-$, with $\frac{3}{2}^-$ unfavored. Thus the spin of the 0.318-MeV level in ^{11}Be is $\frac{1}{2}^-$ ($\frac{3}{2}^-$). The spectroscopic factor[12] obtained for these potentials is about 0.5 for $J^\pi = \frac{1}{2}^-$.

TABLE I. Optical-model parameters used to calculate the curves in Fig. 5.

Entrance channel	Exit channel
$V = 37$ MeV	$V = 55$ MeV
$W = 6.5$ MeV	$W = 6$ MeV
$r_0 = 1.5$ fm	$r_0 = 1.3$ fm
$a = 0.6$ fm	$a = 0.5$ fm

ACKNOWLEDGMENTS

The authors are indebted to Dr. K. L. Englund, formerly of the Hanford, Washington reactor station, for supplying the graphite bars from which the ^{10}Be was extracted. Thanks are due also to D. M. Gordon, whose assistance in burning the graphite and in some of the data taking, is greatly appreciated. We are grateful for helpful comments from Professors T. Lauritsen and T. A. Tombrello.

APPENDIX

A. Extraction of the ^{10}Be

The ^{10}Be was produced by the ^{13}C$(n, \alpha)^{10}$Be reaction in the graphite core of the Hanford, Washington reactor. About 18 kg of natural graphite with an exposure of 3×10^{20} neutrons/cm^2, and having a γ-ray activity of 10 mC, was cut into 1-kg pieces and injected with 1 mC of ^{7}Be tracer. The carbon blocks were burned in an almost pure oxygen environment in a quartz tube with a 10-kW induction heater, as shown in Fig. 6. A small $H_2 + O_2$ flame burning at all times was found to be crucial to the operation, eliminating explosions of carbon dust, and reducing the amount of unburned dust by a factor of 50 when compared with burning without the H_2 flame. The efflux from the furnace passed through a series of several dust traps and filters.

The beryllium was then recovered from the dust and the apparatus using standard chemical techniques, including cation exchange[14] and the solvent extraction procedure of Adam, Booth, and Strickland.[15] The final purification was effected by seven cycles of solvent extraction, wet oxidation,[15] and carrier-free hydroxide precipitation, carried out in equipment constructed entirely of quartz and polypropylene to reduce contamination.

The final result was that 70% of the original ^{7}Be tracer (corrected for five half-lives of decay) was recovered with 1.3 ± 0.1 mg of beryllium. The ratio of ^{10}Be to ^{9}Be was measured by depositing a known fraction of the solution onto a Lucite backing and counting the ^{10}Be β rays in a Geiger counter containing the Lucite. The fraction of the beryllium used was measured by counting γ rays from the tracer. A small correction was made to the β counting rate due to self-absorption in the source. Taking the value[16] for the half-life of ^{10}Be as $(2.7 \pm 0.4)\times10^{6}$ yr, the ratio of ^{10}Be to ^{9}Be is 0.053 ± 0.011. This ratio is close to that expected from irradiation of natural carbon if the ^{12}C$(n, \alpha)^{9}$Be and the ^{13}C$(n, \alpha)^{10}$Be reactions have equal cross sections for neutron energies above the respective thresholds of 6.2 and 4.1 MeV, using an unmoderated fission-neutron energy spectrum.

B. Target Production and Composition

BeF_2 is the only beryllium halide that can be vacuum evaporated after drying from aqueous solution, the other three forming the oxide upon heating. The entire batch of ^{10}Be, 65 μg, was converted to the fluoride, and a small fraction of this was inserted into the platinum boat shown in Fig. 7. Since the electrical contacts are water-cooled, only the center fourth of the platinum boat becomes hot enough to evaporate BeF_2. Typically, about 25% of the material loaded into the boat is deposited upon the foil; the remaining 75% is easily recovered by dissolving in water and reconcentrated without requiring further purification. The platinum foil is then removed and its center is quickly

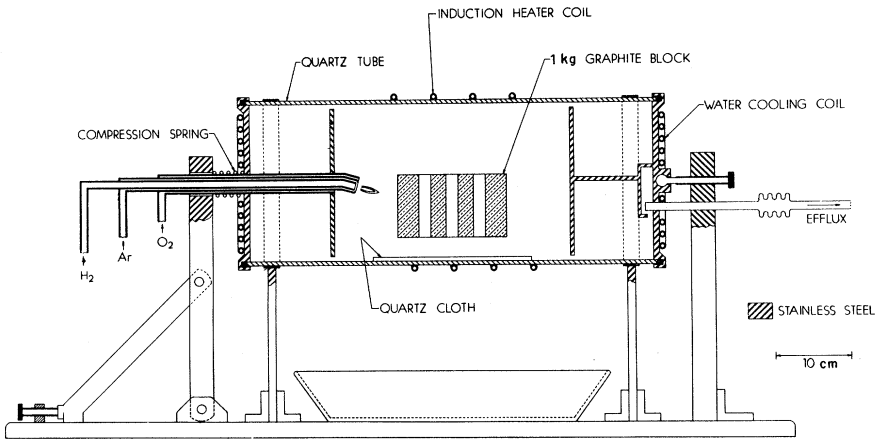

FIG. 6. The induction furnace used to burn the graphite. The block rested on a quartz cloth to reduce thermal stress in the quartz tube. A small flow of Ar gas kept the $H_2 + O_2$ flame away from the tubing. Several air fans were used to cool the apparatus.

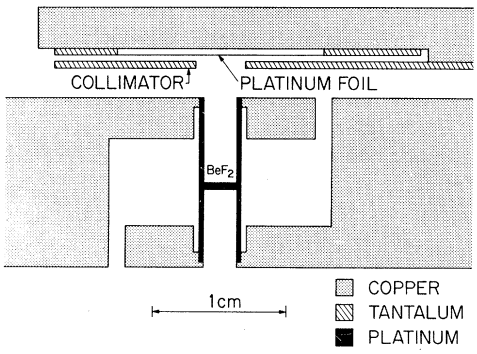

FIG. 7. The platinum boat used to evaporate BeF_2. Steel screws (not shown) clamped the boat to the water-cooled copper electrical contacts. The boat was loaded with BeF_2 in aqueous solution, and the upper copper piece was moved into the position shown after the $BeF_2 \cdot (H_2O)_n$ was dehydrated in vacuum. The tantalum collimator usually caught less than 1% of the BeF_2.

heated in air to 1100°C with an intense collimated light beam, converting the fluoride to the oxide. About 0.2% of the fluorine atoms remain on the target after heating. To obtain uniform targets thicker than about 20 $\mu g/cm^2$, it was found necessary to evaporate a thin layer and bake it in air before evaporating the remainder of the BeF_2.

The spatial distribution of beryllium on the target was measured by observing the 4.44-MeV γ rays from the $^9Be(\alpha, n\gamma)^{12}C$ reaction. The result for an α-particle beam diameter of 0.75 mm is shown in Fig. 8.

For work in which high-energy β rays were detected, commercially rolled platinum foils (5.7 mg/cm^2) were used for the target backings. However, for reactions where protons were detected, thinner Pt foils (about 1 mg/cm^2) were made by vacuum evaporation of Pt from a large W spiral, onto a thin NaCl substrate on glass. In order to produce stress-free Pt films, it was necessary to heat the substrate to about 500°C during the evaporation; otherwise the Pt film would disintegrate upon dissolving the NaCl film. The films so obtained are less dense than annealed Pt, and must be annealed before being subjected to the heating procedure which is used to convert BeF_2 to BeO.

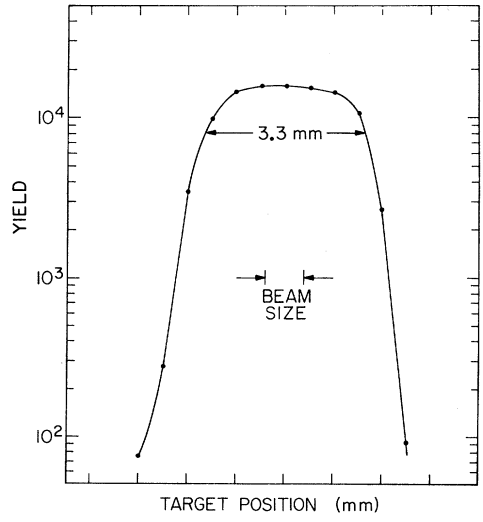

FIG. 8. The spatial distribution of ^9Be on the target, as found from the yield of 4.44-MeV γ rays from the $^9Be(\alpha, n\gamma)^{12}C$ reaction. A cylindrical beam 0.75 mm in diam was used to scan the target vertically.

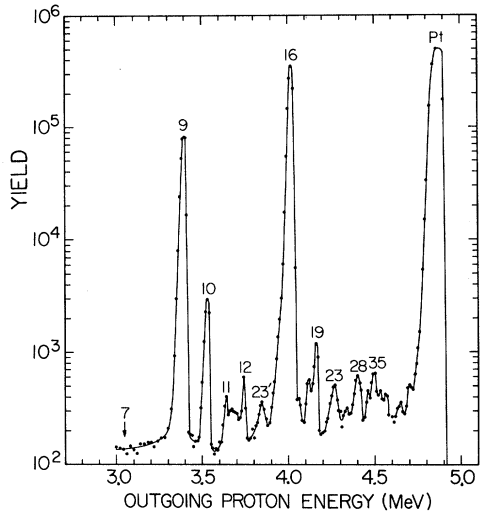

FIG. 9. The energy distribution of elastically scattered protons, taken in reflection geometry for one of the targets. The bombarding energy was $E_p = 5$ MeV, and the magnetic spectrometer was positioned at $\theta_{lab} = 135°$. The approximate abundances of contaminants are listed in Table II. The target was 14 ±2 keV thick to 5-MeV protons. The peaks labeled 23 and 35 are presumably due to residual traces of the NaCl used during the production of the Pt foil. The peak labeled 23′ is attributed to $^{23}Na(p, p')$. The hump between the mass-11 and -12 positions is due to ^{12}C on the back side of the foil.

To check the composition of the BeO targets, a 200 ± 20-$\mu g/cm^2$ target was formed on a 1.2-mg/cm^2 Pt foil, and the elastic-scattering profile (Fig. 9) for 5-MeV protons was measured with the 61-

TABLE II. Target composition.

Isotope	Percent abundance	Method of determination
^{16}O	50.0	chemical
^9Be	47.0	chemical
^{10}Be	2.5 ± 0.5	β counting
^{19}F	~0.4	$^{19}F(p, \alpha\gamma)^{16}O$
^{18}O	0.1	natural abundance ratio
^{11}B	≤0.1	$^{11}B(p, \gamma)^{12}C$
^{10}B	≤0.025	natural abundance ratio

cm-radius magnetic spectrometer. Since the cross sections for elastic scattering from ^{19}F and ^{11}B are not known at this energy, these contaminants were determined by another measurement using $(p, \alpha\gamma)$ and (p, γ) reactions.[17] Table II lists the most abundant contaminants. Since the boron contamination is presumably natural boron, the ratio of ^{10}Be to ^{10}B is thus $\geq$100.

*Supported in part by the National Science Foundation Grant No. GP-9114 and by the Office of Naval Research Contract No. Nonr-220(47).

†Present address: Physics Department, Brookhaven National Laboratory, Upton, Long Island, New York 11973.

[1]D. L. Auton, B. Zeidman, H. T. Fortune, J. P. Schiffer, and R. C. Bearse, Bull. Am. Phys. Soc. 14, 489 (1969).

[2]D. J. Pullen, A. E. Litherland, S. Hinds, and R. Middleton, Nucl. Phys. 36, 1 (1962).

[3]S. Hinds and R. Middleton, Phys. Letters 9, 149 (1964).

[4]D. E. Alburger, C. Chasman, K. W. Jones, J. W. Olness, and R. A. Ristinen, Phys. Rev. 136, B916 (1964).

[5]F. Ajzenberg-Selove and T. Lauritsen, Nucl. Phys. A114, 1 (1968).

[6]M. J. LeVine and P. D. Parker, Phys. Rev. 186, 1021 (1969); J. R. Patterson, H. Winkler, and C. S. Zaidins, *ibid.* 163, 1051 (1967); A. B. McDonald, J. R. Patterson, and H. Winkler, to be published; D. R. Goosman and R. W. Kavanagh, Phys. Rev. 161, 1156 (1967).

[7]J. L. Black, W. J. Caelli, D. L. Livesey, and R. B. Watson, Phys. Letters 30B, 100 (1969).

[8]R. W. Kavanagh, Nucl. Phys. 15, 411 (1960).

[9]T. W. Bonner, A. A. Kraus, J. B. Marion, and J. P. Schiffer, Phys. Rev. 102, 1348 (1956).

[10]D. E. Alburger, E. K. Warburton, A. Gallmann, and D. H. Wilkinson, Phys. Rev. 185, 1248 (1969).

[11]R. H. Bassel, R. M. Drisko, and G. R. Satchler, Oak Ridge National Laboratory Report No. ORNL 3240, 1962 (unpublished).

[12]G. R. Satchler, Nucl. Phys. 55, 1 (1964).

[13]P. E. Hodgson, The Optical Model of Elastic Scattering (Clarendon Press, Oxford, England, 1963).

[14]K. A. Kraus and F. Nelson, in Proceedings of the Conference of the Academy of Sciences of the U.S.S.R. on the Peaceful Uses of Atomic Energy, Moscow, July, 1955 (Akademiia Nauk, S.S.S.R., Moscow, 1955) [English translation by Consultants Bureau, New York: U.S. Atomic Energy Commission Report No. TR-2435 (1956)], Vol. 7, p. 113.

[15]J. A. Adam, E. Booth, and J. D. H. Strickland, Anal. Chim. Acta 6, 462 (1952).

[16]D. J. Hughes, C. Eggler, and C. M. Huddleston, Phys. Rev. 75, 515 (1949).

[17]D. R. Goosman, E. G. Adelberger, and K. A. Snover, Phys. Rev. C 1, 123 (1970).

PHYSICAL REVIEW C VOLUME 1, NUMBER 6 JUNE 1970

Forward Scattering Amplitude with Nuclear Correlations and Overlapping Potentials*

Toshitake Kohmura†

Department of Physics and Astronomy, University of Rochester, Rochester, New York 14627

(Received 8 September 1969)

We have formulated a theory of nuclear scattering for overlapping potentials between the incident particle and each of the target nucleons, without using the impact-parameter approximation of Feshbach. As the nuclear internal Hamiltonian is important for the overlap in the potentials, we include in the energy denominators a term which is dependent on the nuclear internal Hamiltonian, as well as the term which is linear in the momentum transfers. A correction to the Glauber model, due to the overlap in the potentials, is obtained from the principal part of the denominators. The correction reduces both the total cross section and the forward differential cross section by about 15%. We define the "effective solid angle for scattering" to be the total cross section divided by the forward differential cross section. From this quantity we can determine nuclear correlation independently of the correction due to the overlap in the potentials. Range parameters for nuclear correlation functions are obtained from existing data.

1. INTRODUCTION

Nuclear scattering at high energies provides us with information on nuclear structure, such as nuclear correlations, which cannot be obtained from low-energy reactions.[1,2] A number of authors have discussed the possibility of obtaining such correla-